Coherent Ghost Imaging based on sparsity constraint without phase-sensitive detection

2012 EPL 98 24003

(http://iopscience.iop.org/0295-5075/98/2/24003)

A LETTERS JOURNAL EXPLORING THE FRONTIERS OF PHYSICS

April 2012

EPL, **98** (2012) 24003
www.epljournal.org
doi: 10.1209/0295-5075/98/24003

Coherent Ghost Imaging based on sparsity constraint without phase-sensitive detection

Hui Wang[(a)] and Shensheng Han

Key Laboratory for Quantum Optics and Center for Cold Atom Physics of CAS, Shanghai Institution of Optics and Fine Mechanics, Chinese Academy of Sciences - Shanghai 201800, China

received 24 October 2011; accepted 28 March 2012
published online 30 April 2012

PACS 42.30.Wb – Image reconstruction; tomography
PACS 42.30.Va – Image forming and processing
PACS 42.25.Kb – Coherence

Abstract – A universal process for coherent Ghost Imaging (GI) without phase-sensitive detection is presented in this paper. The process is based on the sparsity constraint of the target, which helps to accelerate the information extraction. By taking advantage of this process, the coherent GI scheme with a point-like detector in the test path is improved to achieve higher efficiency and higher resolution, even though the phase information of the random field is lost. This process will contribute to the practical applications, such as Fourier-transform diffraction GI of X-ray, and remote sensing.

Introduction. – Ghost Imaging (GI) is a novel and promising technique that can reconstruct the object's real-space image or its Fourier-transform diffraction spectrum based on the classical or quantum correlation of the light field fluctuations [1,2]. GI has benefited lots of practical applications with its particular scheme advantages [3–6]. However, the traditional GI process of calculating the correlation is little efficient, and massive measurements are required for good visibility.

In fact, the imaging technique is a kind of information extraction, where we are confronted with different information but the very information we are interested in is usually much less than the raw data itself. For a long time, sparsity of the target has been taken as popular *a priori* for information extraction to improve the efficiency [7–9]. The sparsity constraint improves the efficiency by reforming both the algorithms [10,11] and the way of sampling [7,8]. Instead of collecting all the information and processing it, sparsity allows to acquire the useful information with fewer measurements. Sparsity constraint has already been applied to de-noising [12], super-resolution imaging [13–16], and target recognition [17] with success. There are also numerical simulations about the performance of sparsity constraint in quantum state tomography [18].

Recently, efforts have been made to combine GI with sparsity reconstruction [9,16,19,20]. This combination makes great sense because it preserves not only the scheme advantage of GI but also higher efficiency [9] and even super-resolution [19]. Actually, there are two models of GI schemes: incoherent GI and coherent GI [21]. When the test detector of the GI scheme is a bucket-like one that collects all the signal modulated by the target, such as the real-space GI with near-field target, the GI scheme is an incoherent system and a perfect sensing equation can be established by directly using intensities obtained on the test and the reference detectors [9]. However, there are some practical GI schemes where the test detector has to be taken as a point-like one, such as the Fourier-transform diffraction GI and the remote sensing. In such cases, the scheme turns into a coherent system, and the phase information of the light field, which is usually lost during the measuration, will break the perfect sensing equation and further influence the reconstruction. Therefore, a universal process is required to remedy such loss and rebuild a sensing equation for the reconstruction.

In this paper, we propose such a process that can be applied to all kinds of coherent GI schemes based on sparsity constraint. In this process, sparsity constraint allows a more efficient way of compressive sampling, and the known optical scheme and the statistics of light field are taken as extra *a priori* to remedy the lost phase information. Experimental results of diffraction GI via such process are presented to show higher efficiency and higher resolution compared with traditional GI results.

(a)E-mail: ami157@siom.ac.cn

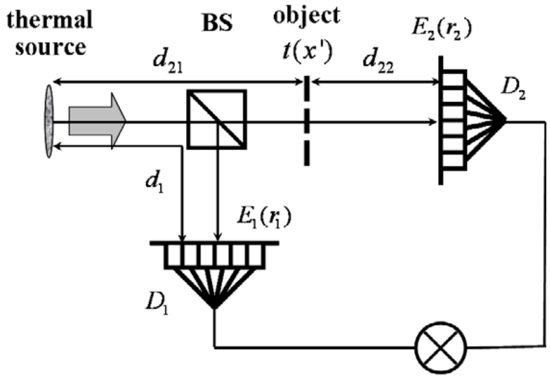

Fig. 1: The scheme of coherent GI . A beam splitter (BS) is introduced to divide the thermal light into two paths: in the reference path, the field propagates freely to an array detector D_1; in the test path, the field modulated by an unknown object is measured by another array detector D_2. The correlation between the intensities on D_1 and D_2 shows the Fourier-transform diffraction spectrum of the object when $d_1 = d_{21} + d_{22}$, or the real-space image of the object when $d_1 = d_{21}$.

Traditional coherent GI. – The scheme of lensless coherent GI is shown in fig. 1 [1,3]. In the traditional GI process, the correlation of intensity fluctuations is calculated between I_1 and I_2 [3,21]:

$$\begin{aligned} G(r_1, r_2) &= \langle I_1(r_1) I_2(r_2) \rangle - \langle I_1(r_1) \rangle \langle I_2(r_2) \rangle \\ &= \left| \int \mathrm{d}x_s I_s(x_s) h_r^*(x_s, r_1) h_t(x_s, r_2) \right|^2, \end{aligned} \quad (1)$$

where r_1, r_2 and x_s represent the transverse position on the reference detector D_1, on the test detector D_2 and on the source plane, respectively, $\langle \cdots \rangle$ represents the ensemble average, $I_s(x_s)$ is the intensity distribution on source plane, $h_r(x_s, r_1)$ and $h_t(x_s, r_2)$ are the impulse response functions in the reference and the test paths, and * denotes the phase conjugate. By substituting different forms of $h_r(x_s, r_1)$ and $h_t(x_s, r_2)$ into eq. (1), the real-space image or the Fourier-transform diffraction spectrum of the object [1,3] can be achieved.

The ensemble average in eq. (1) requires a large number of measurements, which is usually much higher than the pixel number of D_1. This makes GI little efficient. Meanwhile, the finite size of the thermal source $I_s(x_s)$ in eq. (1) introduces the transverse coherent length as the intrinsic resolution limit to GI [22,23].

In Fourier-transform diffraction GI, the spatial averaging technique [21] could be used into eq. (1) for faster convergence:

$$G_{SA}(r) = \sum_{r_2} G(r_1, r_1 + r) \propto \mathrm{const} \times \left| T\left\{ r/(\lambda d_{22}) \right\} \right|^2, \quad (2)$$

where the subscript SA indicates that a spatial average has been carried out, $r = r_2 - r_1$, $T(f) = \frac{1}{2\pi} \int \mathrm{d}x \exp(-i2\pi f x) t(x)$ is the Fourier transform of the object's transmittance function $t(x)$, and λ is the light wavelength.

Obviously, the correlation for different pixels r_1 on D_1 is calculated independently in the traditional process, in other words, the measurement of each pixel is independent.

Coherent GI via sparsity constraint. – Sparsity constraint accelerates the information extraction via compressive sampling, which depends on two principles [7]:

1) the target X is sparse in a certain basis Ψ;

2) the sensing basis Φ is highly incoherent with Ψ.

The sparsity constraint, satisfied by most natural object when expressed in a proper representation basis Ψ, ensures the possibility of compressive sampling and super-resolution [24]. The incoherence between bases Ψ and Φ makes measuration higher efficient [25].

After the sampling, an efficient algorithms is needed for the target reconstruction. In this paper, we resort to the Basis Pursuit (BP) method for the reconstruction [11]:

$$\mathrm{Min} \, \|\mathrm{x}\|_{l_1} \ \text{subject to} \ AX = Y. \quad (3)$$

BP is based on a sensing equation between an unknown object X and the detected signal Y through a known sensing matrix A, where X (N-element) is known to be sparse in basis Ψ. By performing K measurements ($K < N$) in basis Φ, $A = \Phi\Psi$ is a $K \times N$ matrix and Y is a detected K-element vector. In traditional imaging, linear reconstruction is based on measurements in a space with the same dimension as the object, while sparsity allows nonlinear reconstruction from measurements in a space with lower dimension by solving a convex optimization of minimizing l_1-norm [8,26]. Clearly, the measurement for each pixel of X is not independent anymore in this process. All measurements are taken as a whole to relate the high-dimension object space Ψ and the low-dimension sensing Φ.

In fact, the coherent GI scheme itself fits in perfectly with both the compressive sampling and the reconstruction algorithm, which makes it a self-adaptive system under the sparsity constraint: for each measurement, the intensity $I_1(r_1)$ recorded by the detector D_1 is a random vector that could be proved to be largely incoherent with any fixed basis [7]; there is always another point-like detector D_2 in the test path to provide intensity I_2 for a sensing equation about the object X. Accordingly, considering X as sparse in a certain basis, a new imaging process could be developed, where the sensing matrix A is usually related to $I_1(r_1)$, and Y is related to I_2.

In the following part, we take the scheme of lensless diffraction GI ($d_1 = d_{21} + d_{22}$) [3] to demonstrate the process. For each measurement, I_2 could be expressed as

$$I_2(r_2) \propto \int_{obj} \mathrm{d}x\,\mathrm{d}x' E^*(x)E(x')t^*(x)t(x') \times \exp\left\{\frac{i\pi}{\lambda d_{22}}\left[(x-r_2)^2-(x'-r_2)^2\right]\right\}, \quad (4)$$

where $E(x)$ is the field on the object plane, the position integrations of x and x' are over the object plane. To establish a relation between I_2 and I_1, the known information of the GI scheme and light propagation should be taken into account. Consider the array detector D_1 as a large enough conjugate mirror so that the field $E(x)$ on the object plane can be reconstructed by the field $E_1(r_1)$ on D_1, and eq. (4) could be rewritten approximately as

$$\begin{aligned} I_2(r_2) \propto & \int_{ref} \mathrm{d}r_1\mathrm{d}r_1' E_1^*(r_1)E_1(r_1') \int_{obj} \mathrm{d}x\,\mathrm{d}x' t^*(x)t(x') \\ & \times\exp\left\{-\frac{i\pi}{\lambda d_{22}}\left[(x-r_1)^2-(x'-r_1')^2\right]\right\} \\ & \times\exp\left\{\frac{i\pi}{\lambda d_{22}}\left[(x-r_2)^2-(x'-r_2)^2\right]\right\} \\ = & \int_{ref} \mathrm{d}r_1\mathrm{d}r_1' \exp\left\{-\frac{i\pi}{\lambda d_{22}}\left(r_1^2-r_1'^2\right)\right\} \\ & \times E_1^*(r_1)E_1(r_1')T^*\left(\frac{r_1-r_2}{\lambda d_{22}}\right)T\left(\frac{r_1'-r_2}{\lambda d_{22}}\right), \end{aligned} \quad (5)$$

where r_1 and r_1' represent the transversal position on D_1. To be compatible with sparsity reconstruction, eq. (3), eq. (5) could be further discretized for K measurements:

$$\begin{aligned} I_2(r_2^{(k)}) \propto & \sum_{i=1}^{N}\sum_{j=1}^{N} E_1^{*(k)}(r_{1i})E_1^{(k)}(r_{1j}) \\ & \times \exp\left\{-\frac{i\pi}{\lambda d_{22}}(r_{1i}^2-r_{1j}^2)\right\} \\ & \times\Delta r_{1i}\Delta r_{1j}T^*\left(\frac{r_{1i}-r_2^{(k)}}{\lambda d_{22}}\right)T\left(\frac{r_{1j}-r_2^{(k)}}{\lambda d_{22}}\right), \end{aligned} \quad (6)$$

where variables have been discretized $r_1 = \{r_{1i}\}$, $r_1' = \{r_{1j}\}$, $r_2 = \{r_2^{(k)}\}$, $(i, j = 1, \cdots, N; k = 1, \cdots, K)$. Then the sensing matrix A becomes

$$A = \begin{pmatrix} a_{11}^{(1)} & a_{12}^{(1)} & \cdots & a_{ij}^{(1)} & \cdots & a_{NN}^{(1)} \\ a_{11}^{(2)} & a_{12}^{(2)} & \cdots & a_{ij}^{(2)} & \cdots & a_{NN}^{(2)} \\ \vdots & & & \vdots & & \vdots \\ a_{11}^{(k)} & & & a_{ij}^{(k)} & & a_{NN}^{(k)} \\ \vdots & & & \vdots & & \vdots \\ a_{11}^{(K)} & a_{12}^{(K)} & \cdots & a_{ij}^{(K)} & \cdots & a_{NN}^{(K)} \end{pmatrix}, \quad (7)$$

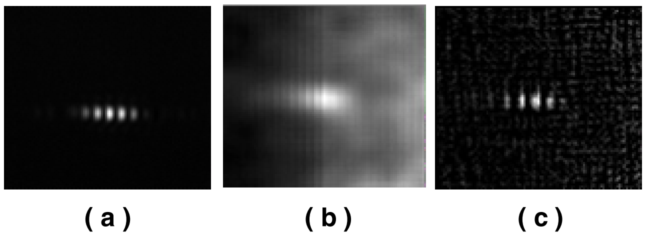

Fig. 2: The experimental spectrum reconstructions $|T(f)|$ of a double slit. (a) spectrum realized by a lens in a f-f system; (b) spectrum by traditional correlated GI with $K = 1000$ measurements; (c) spectrum by sparsity reconstruction (SPGL1) with the same measurements as (b).

where
$a_{ij}^{(k)} \propto E_1^{*(k)}(r_{1i})E_1^{(k)}(r_{1j}) \exp\{-i\pi(r_{1i}^2 - r_{1j}^2)/(\lambda d_{22})\}$.

From eq. (7), if there are N pixels on D_1 and we take K measurements, A should be a $K \times N^2$ matrix. However, for each row of A (each measurement), there are only N elements that can be detected as known intensities $I_1(r_1)$ when $r_1 = r_1'$ or $i = j$, the other $N^2 - N$ mutual-interference elements are in general unobtainable. Fortunately, there is another *a priori* information about the statistics of the light field that can be used for such case.

Since GI uses random thermal source, the phases of the field propagating in the scheme obey uniform random distribution with zero average value. Based on such statistics, the phase distribution of $E_1^{(k)}(r_1)$ can be properly conjectured to be $\varphi^{(k)}(r_1)$ for the k-th measurement to establish a $K \times N^2$ matrix A. Although the conjectured phases $\varphi^{(k)}(r_1)$ deviate from the true values, since we only care about the N elements of $|T(f)|$, the deviations can be compensated by the phase of $T(f)$, which are less important in our case.

Till now, it seems like we establish an equation in sacrifice of calculation cost by expanding A from $K \times N$ to $K \times N^2$. In fact, it shows we can do much better than that. Since the random conjectured phases make the $N^2 - N$ mutual-interference terms easily counteracted during the summation in eq. (6), the N known intensities play dominant roles over the $N^2 - N$ mutual-interference ones. This means that it is not necessary to conjecture all the $N^2 - N$ phases, conjecturing only part of them will be enough. Actually, there is a tradeoff between the number of conjectured phases and convergence. Less conjectures will decrease the calculation cost but lead to a slower convergence that requires more measurements. Spatial average can also be applied in such case to enhance the convergence.

Experimental results. – Experimental reconstructions are shown in fig. 2 and fig. 3. The schemes are the same as shown in fig. 1 with $d_{21} = 20\,\mathrm{cm}$, $d_{22} = 5\,\mathrm{cm}$, $d_1 = 25\,\mathrm{cm}$. The pseudo-thermal source is realized by passing a laser beam through a slowly rotating ground glass disk. The source size is $\sigma = 3\,\mathrm{mm}$ with $\lambda = 0.532\,\mu\mathrm{m}$.

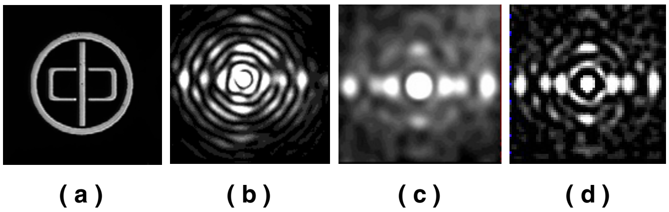

Fig. 3: The experimental spectrum reconstructions of a "Zhong" ring. (a) The object; (b) spectrum realized by a lens in a f-f system; (c) spectrum by traditional GI with $K = 4000$ measurements; (d) spectrum by sparsity reconstruction (GPSR), with the same measurements as (c).

In fig. 2, the object is a double slit with slit width 200 μm and slit separation 600 μm. The Fourier spectrum shown in fig. 2(a) is realized by using a lens (focus = 5 cm) in a f-f system. The GI reconstruction by intensity correlation and by BP are shown in fig. 2(b) and (c), respectively. The pixel number of the image is $N = 100 \times 100 = 10000$, and there are only 10000 terms of $E_1(r_{1i})E_1(r_{1j}), (i \neq j)$ with conjectured phases in each measurement. Spectral Projected Gradient for l_1-norm minimization (SPGL1) is used here for BP problem in eq. (3), where we assume the spectrum is sparse in real space.

Figure 3 shows the spectrum reconstruction of a "Zhong" ring with diameter 0.8 mm. Here $N = 64 \times 64 = 4096$, we consider all $N^2 - N$ mutual-interference terms to be zero and only use the measured N intensities $I_1(r_1)$ for the reconstruction. Gradient Projection for Sparse Reconstruction (GPSR) is used here to solve eq. (3), where we take the Discrete Cosine Transform (DCT) basis as the sparse basis.

In fig. 2 and fig. 3, both traditional GI process and sparsity reconstructions have been performed through spatial average technique [21]. Obviously, reconstructions with sparsity constraint obtain higher visibility and higher resolution than traditional GI. Both successful reconstructions show the feasibility of this process with a reasonable calculation cost. The comparison between the measurement number of fig. 2 and fig. 3 also shows the tradeoff between the number of conjectured phases and the convergence.

In conclusion, we demonstrate a universal process for coherent GI based on sparsity constraint. In this process, the knowledge of the imaging scheme, the light propagation and the statistics of light field should also be considered as *a priori* information for the sparsity reconstruction. This technique opens up a new approach to nonlocal GI systems with higher efficiency and higher resolution, which could be applied in diffraction imaging of X-ray and remote sensing [4].

* * *

The work is supported by the National High Technology Research and Development Program of China (863 Program) No. 2011AA1201, National Natural Science Foundation of China under Grant Project No. 60877009, and Shanghai Natural Science Foundation under Grant Project No. 09JC1415000.

REFERENCES

[1] Basano Lorenzo and Ottonello Pasquale, *Appl. Phys. Lett.*, **89** (2006) 091109.
[2] Gatti A., Brambilla E., Bache M. and Lugiato L. A., *Phys. Rev. A*, **70** (2004) 013802.
[3] Cheng Jing and Han Shensheng, *Phys. Rev. Lett.*, **92** (2004) 093903.
[4] Gong Wenlin, Zhang Pengli, Shen Xia and Han Shensheng, *Appl. Phys. Lett.*, **95** (2009) 071110.
[5] Gong Wenlin and Han Shensheng, *Opt. Lett.*, **36** (2011) 394.
[6] He Shibei, Shen Xia, Wang Hui, Gong Wenlin and Han Shengsheng, *Appl. Phys. Lett.*, **96** (2010) 181108.
[7] Candès E. J. and Wakin M. B., *IEEE Signal Process. Mag.*, **25** (2008) 21.
[8] Romberg J., *IEEE Signal Process. Mag.*, **25** (2008) 14.
[9] Katz O., Bromberg Y. and Silberberg Y., *Appl. Phys. Lett.*, **95** (2009) 131110.
[10] Tropp Joel A., *IEEE Trans. Inf. Theory*, **50** (2004) 2231.
[11] Chen Shaobing Scott, *Basis Pursuit*, PhD Thesis, Department of Statistics, Stanford University, `http://playfair.stanford.edu/~schen/` (1995).
[12] Villaron Emilie, Anthoine Sandrine and Torrésani Bruno, in *Proceedings of SPARS11: 4th Workshop on Signal Processing with Adaptive Sparse Structured Representations Edinburgh, UK, June 2011*, p. 28, `http://ecos.maths.ed.ac.uk/SPARS11/`.
[13] Zweig G., *IEE Proc. Radar Sonar Navig.*, **150** (2003) 247.
[14] Shechtman Yoav, Gazit Snir, Szameit Alexander, Eldar Yonina C. and Segev Mordechai, *Opt. Lett.*, **35** (2010) 1148.
[15] Gazit Snir, Szameit Alexander, Eldar Yonina C. and Segev Mordechai, *Opt. Express*, **17** (2009) 23920.
[16] Wang Hui, Han Shensheng and Kolobov Mikhail I., in *Proceedings of SPARS11: 4th Workshop on Signal Processing with Adaptive Sparse Structured Representations, Edinburgh, UK, June 2011*, p. 109, `http://ecos.maths.ed.ac.uk/SPARS11/`.
[17] Stojanovic I. and Karl W. C., *IEEE J. Sel. Top. Signal Process.*, **4** (2010) 164.
[18] Gross David, Liu Yi-Kai, Flammia Steven T., Becker Stephen and Eisert Jens, *Phys. Rev. Lett.*, **105** (2010) 150401.
[19] Gong Wenlin and Han Shensheng, arXiv:0911.4750v2 [quant-ph] (2010).
[20] Liu Jiying, Zhu Jubo, Lu Chuan and Huang Shisheng, *Opt. Lett.*, **35** (2010) 1206.
[21] Bache M., Brambilla E., Gatti A. and Lugiato L. A., *Opt. Express*, **12** (2004) 6067.
[22] Zhang Pengli, Gong Wenlin, Shen Xia, Huang Dajie and Han Shensheng, *Opt. Lett.*, **34** (2009) 1222.
[23] Gatti A., Bache M., Magatti D., Brambilla E., Ferri F. and Lugiato L. A., *J. Mod. Opt.*, **53** (2006) 739.
[24] Donoho David L., *STAM J. Math. Anal.*, **23** (1992) 1309.
[25] Candès E. and Tao T., *IEEE Trans. Inf. Theory*, **52** (2006) 5406.
[26] Boyd S. and Vandenberghe L., *Convex Optimization* (Cambridge University Press) 2004, pp. 127–146.